

Effect of Marangoni Induced Flow on the Rate of Refractory Dissolution in Molten Slags

K.O.Fagerlund¹, S. Sun and S. Jahanshahi

¹Visiting scientist from Helsinki University of Technology,
Laboratory of Metallurgy, Box 6200, FIN-02015 HUT, Finland
Fax: (+358 9) 451 2798

GK Williams CRC for Extractive Metallurgy,
CSIRO Minerals,
Box 312, Clayton South, VIC 3169, Australia
Fax: (613) 9562 8919

Keywords: Marangoni effect, mass transfer, iron silicate slag, refractory

ABSTRACT

Dissolution of silica rods in 15-30%SiO₂-containing iron-saturated silicate slags was measured using the rotating cylinder technique at 1300°C, under a controlled atmosphere of deoxidised Ar-gas. These measurements were aimed at quantifying the magnitude of Marangoni induced flow near the slag-refractory region. The Marangoni effect was found to be significant under stagnant conditions, but gradually became dominated by bulk flow when the linear velocity of the flowing melt was increased, and reached values in the range of 0.09-0.16 m/s. This implies that, in highly agitated vessels, the Marangoni effect is unlikely to play a dominant role in refractory wear at the slag line. Also, the silica dissolution rate and mass transfer coefficient were examined, and it was found that with increasing silica content of the slag, the dissolution rate and mass transfer coefficient decreased. Furthermore, the relationship between Marangoni number and Reynolds number was calculated, and boundary flow conditions determined using the experimental critical velocity.

1. INTRODUCTION

It has been shown for aqueous systems, that non-reacting surface-active solutes can retard mass transfer and hence reaction, by impeding surface renewal. But, the surface-active solutes, which enter into reactions, may speed up surface renewal and accelerate reaction by causing turbulence in the interfacial region¹⁾. In metal and slag systems densities and dynamic viscosities up to an order of magnitude greater than aqueous systems are not uncommon. There are also considerable differences in surface tension. There exists an effect, known as interfacial turbulence caused by a surface tension gradient, and it is considered to increase the mass transfer in molten slag-metal systems. This effect was probably first investigated by Thompson in 19th century²⁾ and later investigated and published by Marangoni (1840-1925)³⁾. This type of interfacial turbulence became known as "Marangoni flow", and is usually observed in the presence of non-uniform surface tension regions.

Surface or interfacial tension gradient on the surface of liquid may be caused by the gradients of temperature T , concentration c of the surface-active component and electric potential ψ at the interface. This gradient leads to a shear stress, written as

$$t_s = \frac{ds}{dx} = \frac{\partial s}{\partial T} \cdot \frac{dT}{dx} + \frac{\partial s}{\partial c} \cdot \frac{dc}{dx} + \frac{\partial s}{\partial \psi} \cdot \frac{d\psi}{dx} \quad (1)$$

In hydrodynamics this surface tension gradient is called the "Marangoni effect". As mentioned previously, liquid metals and slags generally have high surface or interfacial tensions and also strong surface-active components present, such as oxygen and sulfur, in which case both factors are favourable for occurrence of Marangoni induced flow.

It is a well-known fact that oxide refractories are locally corroded at the slag-gas or slag-metal interface in contact with high temperature melts. For instance, Mukai has made several investigations of local corrosion of refractories by liquid slag at the slag surface caused by active motion of slag, and according to his study on $FeO-SiO_2$ -system⁴⁾, the slag film motions for a rod and prism specimen immersed in $FeO-SiO_2$ slag are demonstrated in Fig.1. This slag film motion is believed to be induced by the Marangoni effect. When an interface between two immiscible fluids is subjected to a concentration or temperature gradient, its interfacial tension varies, and these gradients along the surface induce shear stresses that result in fluid motion. This phenomenon, which is caused by the active motion of slag film, is usually linked to the Marangoni effect in the vicinity of the interface. The velocity profile can attain a maximum velocity from some mm/s to several cm/s, depending on the surface tension, temperature coefficient and liquid viscosity⁵⁾. This can lead to detrimental dissolution of refractory at the metal-slag-gas interface. However, intensive agitation is common in many smelting vessels and the relative role of Marangoni induced flow in comparison to bulk liquid flow in practical smelting systems has not been reliably established. Most of the attempts to model fluid flow in smelting vessels neglect the importance of Marangoni flows at the slag-gas interface. Studies by Broadbent et al.⁶⁾ illustrate that better simulation of heat and fluid flow in furnaces is required, and since there is a lack of knowledge in interfacial tension values, quantitative data on the magnitude of these flows is necessary. Therefore, in order to clarify the contribution of the Marangoni effect, and to distinguish between Marangoni and agitated flow induced refractory dissolution, rotation experiments were conducted.

2. EXPERIMENTAL

Iron saturated iron silicate slags were prepared from pre-dried mixtures of metallic iron (Fe), ferric oxide (Fe_2O_3) and silica (SiO_2), milled to obtain a homogenous mixture, and melted in iron crucibles (50 mm OD, 36 mm ID, and 50 mm height). The compositions of the prepared slags are shown in Table 1. 100 g of dried and milled slag was used in each experiment.

Experiments were carried out in a vertical tube furnace heated with MoSiO_2 elements. The temperature of the melt and the sample was measured using R-type thermocouples. In each experiment, the furnace tube was first flushed with argon, the crucible containing the slag was placed in the hot zone and heated to the 1300°C , at the rate of $6^\circ\text{C}/\text{min}$, under an atmosphere of argon gas. The molten slag was then allowed to homogenise for 2 h before introduction of the silica rod. At the beginning and end of each experiment the melt was sampled by dipping a mild steel rod into the molten slag, and quenching the slag in water. Chemical analyses of the slag samples are given in Table 1.

Experiments were carried out under a controlled atmosphere of purified argon, which was passed through columns of silica gel and anhydrous magnesia perchlorate to remove moisture, and through copper turnings at 500°C to remove oxygen. A mass flow controller was used for controlling the flow of the gas, which was about 1.6 l/min during heating and reduced to 1 l/min after having reached the desired temperature. Translucent silica rods of 12 mm outer diameter were immersed into molten slag (~ 3 cm deep) at a predetermined rotation speed and time, and then lifted from the molten slag to the cooler section of the furnace.

The experimental set-up is shown schematically in Fig. 2, where the local corrosion zone and slag film movement has been illustrated. The values for dissolution rate, R_1 , R_2 , (radius decrease: 1 at the surface and 2 below the surface) Δm (weight loss) and ΔV (volume difference), were measured. Critical rotation velocity, V_{cr} , was determined from the interception point of two lines, R_1 and R_2 against rotation velocity. Dissolved silica samples were photographed using a Kodak DC 240 digital camera, weight loss and volume difference was determined, and the samples were then prepared for microscopic studies. Samples were mounted in resin, cut cross-sectionally and polished. Measurements for the sample radius were made using Vernier callipers and optical microscope. Quantitative analyses were carried out using a scanning electron microscope equipped with an energy dispersive spectrometer.

3. RESULTS AND DISCUSSION

An example of a side view of fused silica rods before and after the test in molten Fe-saturated silicate slag 3 is shown in Fig. 3. Where, a small amount of silica saturated slag formed on the surface and was attached on the rod. The silica dissolution rate appears to vary along the rod length, and is highest at the slag surface with low rotation speed. The preferential attack at the slag line was believed to be due to the Marangoni effect, i.e., the surface being pulled from the rod and inducing an upward slag flow along the rod surface in the vicinity of the gas-solid-liquid contact region. However, once the agitation of bath reaches a certain limiting velocity, the visible necking effect seems to disappear.

Sample profile from the interface and below the melt surface was measured using Vernier callipers and optical microscope. Using the average values for R_1 and R_2 , and evaluating the interception point of regression lines, the critical rotation velocity, V_{cr} , can be determined from graphs shown in Fig. 4. This value was estimated to be, $V_{\text{cr}} = 8.8, 15$ and 16.2 cm/s for

slags 1, 3 and 4, respectively. Results obtained with slag 2 were too scattered to allow the derivation of V_{cr} with certainty, and further confirmation is needed.

3.1 Effect of surface-active agent

Despite the uncertainties in the reported surface tensions of iron silicate, it is quite clearly established that the surface tension of FeO_x - SiO_2 slag is decreased by the dissolved SiO_2 ⁷⁻¹²⁾, as is shown in Fig. 5. It is suggested that the surface activity of SiO_2 is most significant in melts containing less than 5% Fe_2O_3 , corresponding to iron saturated conditions⁷⁾. A positive temperature coefficient (dy/dT) has been reported in slags with 30% SiO_2 content, and Mills and Keene⁷⁾ suggested that this behaviour may be associated with the presence of bridging oxygen on the surface.

In Figure 6, the critical velocity, V_{cr} , is plotted versus the SiO_2 content of the slag. V_{cr} can be seen to increase with increasing SiO_2 , from 15 to 30%. Intuitively, however, when SiO_2 in bulk slag increases, the concentration gradient on the surface near the contact with silica rod would decrease, resulting in a lower surface tension and therefore a lower driving force for Marangoni flow. In this case, a lower V_{cr} would be expected. In other words, the critical bulk flow velocity required to overshadow the Marangoni induced flow would be lower. This is obviously the opposite trend as depicted by the data shown in Fig. 6.

This disagreement could largely be the result of uncertainties in determination of V_{cr} . Other possible reasons may include differences in the mass transfer rates across the boundary layer in the bulk flow versus that in Marangoni induced flow. In particular, the boundary layer in the latter case may be much thinner and not as sensitive to the viscosity as for the bulk flow. Furthermore, the surface tension gradient responsible for the flow near the solid surface may be restricted within a short distance and insensitive to the bulk SiO_2 concentration. Obviously, more experimental work is required to clarify the given trend in Fig. 6.

3.2 Industrial vessels

Gas-induced agitation plays a critical role in promoting mass transfer in many pyrometallurgical operations, both in non-ferrous and ferrous smelting. The flow conditions inside metallurgical vessels are highly complex and there are not many published velocity measurements on hot melts, however, computational fluid flow modelling and water models give some idea of the magnitude of velocity profile. The dominant non-ferrous converting method, Pierce-Smith, uses submerged high velocity gas injection, which causes severe refractory-wear, particularly around the tuyere line. This method achieves flow rates of molten slag in the vicinity of refractory of up to 0.2-2 m/s²¹⁾. Hejja and Eric²²⁾ have reported the velocity of slag in electric matte smelting furnaces as 0.002 m/s, obtained by measurements under operating conditions. This flow is radially directed away from the surface of the electrode on the top of the slag, and is an order of magnitude higher in the transverse flow direction than in the axial bulk flow direction²²⁾. In recent years there has been increased interest in development of high intensive smelting processes, which employ gas injection at high flow rates, such as iron smelting-reduction process, HIs melt²³⁾, and the non-ferrous submerged combustion process, Sirosmelt²⁴⁾. Maximum downward velocity at the wall in a Sirosmelt reactor can reach molten flow rates of up to 0.4-0.9 m/s²⁵⁾, and is naturally dependant on design and many operating parameters, such as blowing rate, lance position, vessel geometry etc. For an early version of HIs melt using bottom injection, velocity around 0.5 m/s near the wall has been published²⁶⁾. In general the maximum velocity

profile in the slag-refractory interface range 0.1-1 m/s²⁶⁾. Themelis et al.²⁷⁾ have examined the gas-injected Slag Resistance Electric Furnace (SRF) for zinc recovery from slags. The calculated velocity profiles using FIDAP program shows the maximum velocity profile pointing downwards alongside the wall, giving an approximate maximum value of 0.17 m/s.

Experimentally determined critical velocities in this study range from 0.09-0.16 m/s. These values indicate that, apart from non-agitated electric furnaces, stirring in metallurgical vessels, such as PS-converters, HIs melt, and SRF, might have a relatively larger effect on refractory erosion than Marangoni induced flow in the slag line. Although, the critical velocity results in this study may not be directly comparable to industrial smelting vessels, they provide a reference for comparison, when balancing the surface-active agents in slag, and stirring or agitation in bath. This information may give some guideline for assessing whether Marangoni flow or bath agitation is primarily responsible for refractory erosion. Since in practical smelting, slag movement in the bath can easily attain velocity of the order of m/s, the liquid flow due to bulk agitation is most likely to dominate the refractory wear at the slag line.

3.3 Mass transfer

The results shown in Fig. 7 (a) and (b) suggest that the rate of dissolution may be controlled by mass transfer in the slag phase. The mass transfer coefficient, k , is calculated from the experimental data (eq. 2), and using dimensionless correlations by Eisenberg et al.,¹³⁾ Olsson et al.,¹⁴⁾ (eq. 3). Density, viscosity and diffusivity data for FeO-Fe₂O₃-SiO₂ slag compositions were taken from literature values^{15-19,28)}. Neglecting any decrease in rod diameter, the calculated mass transfer coefficient values are shown in Fig. 7(a) and (b). Silica saturation (~38.5%SiO₂) is estimated from the iron-silica-saturated boundary at 1300°C and experimental and calculated mass-transfer coefficients are compared in Fig. 7(a). Effect of concentration gradient of SiO₂ on k , using the following assumptions, is shown in Fig. 7(b). Since the sample surfaces are generally not smooth or geometrically easily interpreted, the amount of silica dissolved, $-dr/dt$, was estimated from the mass loss, density and immersion depth. Also, the assumption was made that the interface between the sample rod and the bulk slag is saturated with silica, and therefore liquid composition corresponds to equilibrium bath temperature. Under these conditions experimental mass-transfer coefficient was determined by using the equation:

$$k = - \frac{\mathbf{r}}{M \cdot \Delta c} \cdot \frac{dr}{dt} \quad (2)$$

Calculated mass-transfer coefficient was estimated by equation¹³⁾:

$$k = 0.079 \cdot V^{0.7} \cdot D_r^{-0.3} \cdot \mathbf{r}^{0.344} \cdot \mathbf{m}^{-0.344} \cdot D^{0.644} \quad (3)$$

Where: M is average molecular weight of slag, Δc surfactant concentration difference, ρ density of silica, k is mass transfer coefficient, $-dr/dt$ is the average rate of the sample radius decrease, V is the linear velocity of rotating rod, D diffusivity taken from literature²⁰⁾, and D_r is a diameter of the rod. In a dissolution process which is limited by diffusion, the solid is dissolved by the mutual diffusion of the solute and solvent, and equation (3) has been proposed by Olsson et al.¹⁴⁾ to describe the steady-state rate of movement, due to dissolution, of an interface in a binary liquid-solid system. The boundary layer thickness, $\delta = D/k$, can be

estimated from the diffusivity, D , and experimental mass transfer coefficient, k . The increasing boundary layer thickness with increasing silica in slag, shown in Table II, can be expected from the dissolution rate, and mass transfer coefficient values. In this calculation, a constant value of $5 \times 10^{-6} \text{ cm}^2/\text{s}$ was used for the diffusivity of SiO_2 . Physical properties of slags used for the calculations were found to be somewhat inconsistent, thus the calculated theoretical values given in this report should be studied with some caution.

3.4 Effect of Marangoni number on Reynolds number

The dimensionless Marangoni number, Ma , is defined as³⁾:

$$Ma = (L_s \cdot \rho \cdot c_p \cdot \delta \gamma) / (\lambda \cdot \mu), \quad (4)$$

where L_s is a characteristic length, ρ is the density, C_p is the specific heat, $\delta \gamma$ is the difference in surface tension along L_s , λ is the thermal conductivity, and μ is the viscosity. The experiments of the present work were carried out at a constant temperature, 1300°C . Assuming isothermal conditions, the Marangoni effect may be considered to be purely due to a chemical gradient, for example in this case SiO_2 concentration. In this work we define a dimensionless Marangoni number describing convection, when a surface tension variation arises from concentration gradient as

$$Ma = \frac{dg \cdot L_s}{D \cdot m} \quad (5)$$

where D is the diffusivity of SiO_2 in slag. Characteristic length L_s was chosen to be a boundary layer thickness, $\delta = D/k$, that can be estimated from the diffusivity and mass transfer coefficient, as previously mentioned.

Reynolds number is used as a criterion for flow transition and has a dimensionless quantity given by

$$R_e = \frac{L \cdot V \cdot \rho}{\mu} \quad (6)$$

Characteristic length, L , while calculating Re number, was chosen to be the radius of the rotating sample R . The surface tension difference was estimated from the literature values⁷⁻¹²⁾, and assuming that the interface between sample and bulk slag is saturated with silica, the concentration gradient corresponds to equilibrium bath temperature and chemical melt composition.

The experimental and calculated results are plotted in the Re - Ma plane in Fig. 8. Calculated mass transfer coefficient was estimated by equation (3) in Fig. 8 (a) and experimentally determined by equation (2) in 8 (b). For a given slag, the Reynolds number, Re , increases with the rotation speed in both figs., as expected. The Marangoni number, Ma , decreases due to apparent decrease in the boundary layer thickness in the slag. The critical Re , corresponding to V_{cr} for slags 1,3 and 4, are shown in these Figures. The critical Reynolds number is positively correlated to Marangoni number. In other words, as Marangoni flow intensifies, the critical bulk flow, characterised by $LV\rho/\mu$, will also increase, although V_{cr} decreases.

4. CONCLUSIONS

The significance of Marangoni induced flow in agitated bath conditions to refractory dissolution was studied by rotational experiments on Fe-saturated silicate melts at 1300°C. The following conclusions were made. The magnitude of the Marangoni effect was found to be significant under stagnant conditions, but became dominated by bulk flow when the linear velocity of the flowing melt reached values in the range of 0.09-0.16 m/s. The critical Reynolds number is found to increase with increasing Marangoni flow, although critical velocity decreases. The relatively minor magnitude of the critical velocity, $V_{cr} \sim 0.09-0.16$ m/s, implies that in highly agitated vessels, the Marangoni effect may not be a predominant cause for refractory wear at the slag line.

5. ACKNOWLEDGMENTS

Financial support for this work was provided by G.K.Williams Cooperative Research Centre for Extractive Metallurgy, a joint venture between CSIRO Minerals and The University of Melbourne, Department of Chemical Engineering. The authors also thank the Academy of Finland, the Walter Ahlström Foundation, the Foundation for Research of Natural Resources in Finland and the Outokumpu Foundation. The authors gratefully acknowledge the assistance in experimental work by J. Bremmel and R. Davidson.

6. REFERENCES

1. Richardson, F.R. Interfacial phenomena and metallurgical processes. Canadian Met. Quart. Vol 21, No 2, 1982, 111-119.
2. Thompson. J. Phil. Mag. 10, 1855, 330.
3. Marangoni, C. Annal. Phys. Poggendorff 143, 1871, 337; Nuovo Cim. 5/6, 1871, 293; 3, 1978, 97.
4. Yu, Z. and Mukai, K. Direct Observation of the Local Corrosion of Solid Silica at the Surface of Liquid Fe₂O-SiO₂ Slags. J. Japan. Inst. Metals, 56(10)1992, 1137-1144.
5. Ricci, E. Nanni, L. and Passerone, A. Oxygen transport and dynamic surface tension of liquid metals. In: Marangoni and Interfacial Phenomena in Materials Processing, Discussion of the Royal Society of London, UK, 1998, 43-55.
6. Broadbent, C.P. Tsotridis, G. and Hondros, H. The Influence of Marangoni Interfacial Flows in Flux-Line Erosion. 4th International Conference on Molten Slags and Fluxes, Sendai, ISIJ, 1992, 370-373.
7. Mills, K.C. and Keene, B.J. Intl. Materials Rev. 32, 1987, 1.
8. Kawai, Y. Mori, K. Shiraishi, H and Yamada, N. Surface Tension and Density of FeO-CaO-SiO₂ Melts. Tetsu-to-hagane (J. Iron Steel Inst. Jpn.), Vol. 62, 1976, 53-61.

9. Kidd, M. and Gaskell, D.R. Measurement of the Surface Tensions of Fe-Saturated Iron Silicate and Fe-Saturated Calcium Ferrite Melts by Padday's Cone Technique. *Met. Trans.*, Vol 17B, December 1986, 771-776.
10. King, T.B. The Surface tension and Structure of Silicate Slags. *J. Soc. Glass Technology*, Vol 35, 1951, 241-59.
11. Kozakevitch, P. Tension superficielle et viscosite des scories synthetiques. *Rev. Met.* Vol 46, 1949, 8, 505-16.
12. Popel, S.I. and Esin, O.A., *Zh. Fiz. Khim.*, Vol 30, 1956, 1193-1201.
13. Eisenberg, M., Tobias, C.W. and Wilke, C. R., Mass Transfer at Rotating Cylinders. *Chem. Eng. Prog., Symp. Ser.*, vol 51, 1955, 1-16.
14. Olsson, R.G., Koump, V. and Perzak, T.F., Rate of Dissolution of Carbon-Steel in Molten Iron-Carbon Alloys. *Trans. Met. Soc. AIME*, vol 233, 1965, 1654-1657.
15. Verein Deutscher Eisenhüttenleute, Ed., *Slag Atlas*, (Verlag Stahleisen GmbH, D-Dusseldorf, 2nd edition, 1995), 616.
16. Mills, K.C. and Keene, B.J., Physical properties of BOS slags. *Int. Materials Reviews*. Vol 32, 1987, 1-120.
17. Utigard, T.A. and Warczok, A. Density and Viscosity of Copper/Nickel Sulphide Smelting and Converting Slags. In: *Pyrometallurgy of Copper*, The Metallurgical Society of CIM, Santiago, Chile, 1995, 423-437.
18. Zhang, L. and Jahanshahi, S. Review and Modelling of Viscosity of Silicate Melts: Part II. Viscosity of Melts Containing Iron Oxide in the CaO-MgO-MnO-FeO-Fe₂O₃-SiO₂ System. *Met. Trans.* Vol. 29B, 1998, 187-194.
19. Turkdogan, E.T., *Physicochemical properties of molten slags and glasses*. The Metals Society, London, 1983, 516.
20. Asaki, Z. Chiba, Y. Oishi, T. and Kondo, Y. Kinetic Study on the Reaction of Solid Silica with Molten Matte. *Met. Trans. B*(21B), 1990, 19-25.
21. Vaarno, J., Pitkala, J., Ahokainen, T. and Jokilaakso, A. Modelling Gas Injection of a Peirce-Smith Converter. *Inter Conf on CFD in Mineral & Metal Processing and Power Generation*. Melbourne, Australia, CSIRO 1997, 297-306.
Vaarno, J. Private communication, Outokumpu Research Oy, October 1999.
22. Hejja, A.A. and Eric, R.H., *EPD Congress 1996*, ed., Warren, G.W., The Minerals, Metals & Materials Society, 1995, 27-41.
23. Innes, J.A. Moodie, J.P. Webb, I.D. and Brotzmann, K. 7th Process Technology Division Conference, ISS/AIME, 1988, 225-231.

24. Rankin, W.J. Jorgensen, F.R.A. Nguyen, T.V. Koh, P.T.L, and Taylor, R.N. Process engineering of SIROSMELT reactors: lance and bath-mixing characteristics. Extraction Metallurgy '89, IMM, 1989, 577-600.
25. Nguyen, T.V. Private communication, CSIRO Minerals, October 1999.
26. Schwarz, P. The Role of Computational Fluid Dynamics in Process Modelling. 6th AusIMM Extractive Metallurgy Conference, Brisbane, Australia, 3-6 July 1994, 31-36. Schwarz, P. Private communication, CSIRO Minerals, January 2000.
27. Themelis, N.J. Peacey, J.G. and Jiao, Q. Recovery of zinc in a slag resistance electric furnace. Proceedings of H.H.Kellogg International Symposium, ed. N.J.Themelis and P.F.Duby, Warrendale, PA: The Metallurgical Society, 1991, 331
28. Goto, K.S. and Ukyo, Y., The interdiffusivity matrix of $\text{Fe}_2\text{O}_3\text{-CaO-SiO}_2$ melt at 1693 to 1773°K. Metall. Trans. B, 12B., 1981, 449-454.

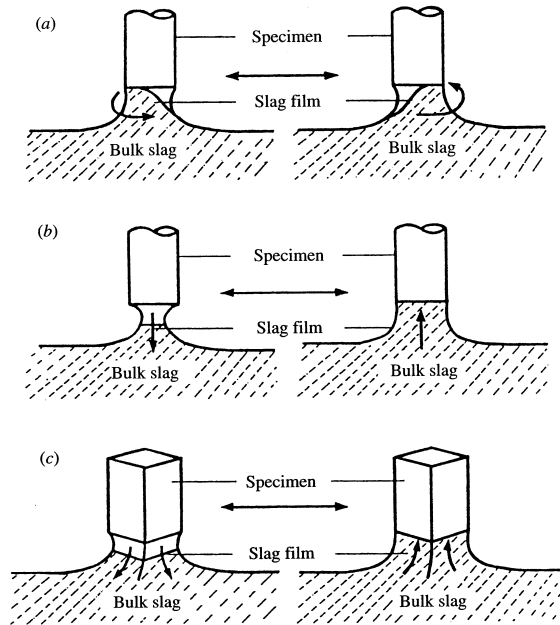


Figure 5. Slag film movements for rod and prism silica specimens dipped in a $\text{Fe}_t\text{O-SiO}_2$ slag (Yu & Mukai 1992): (a) rotational movement of slag film for the rod specimen; (b) up-and-down movement of slag film for the rod specimen; (c) up-and-down movement of slag film for the prism specimen.

Figure 1. Slag film movement for silica rod and prism in $\text{Fe}_t\text{O-SiO}_2$ slag according to Yu and Mukai⁵⁾.

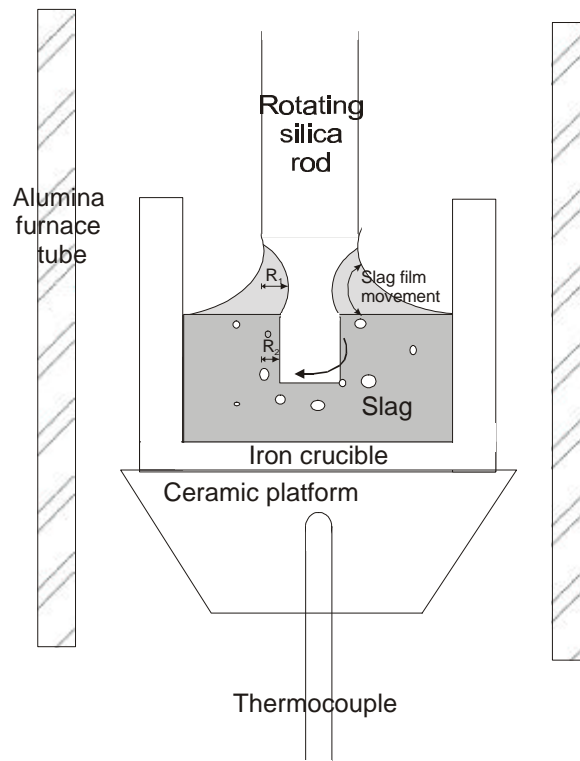


Figure 2. Schematic presentation of the silica rod rotated in a molten Fe-saturated silicate slag.

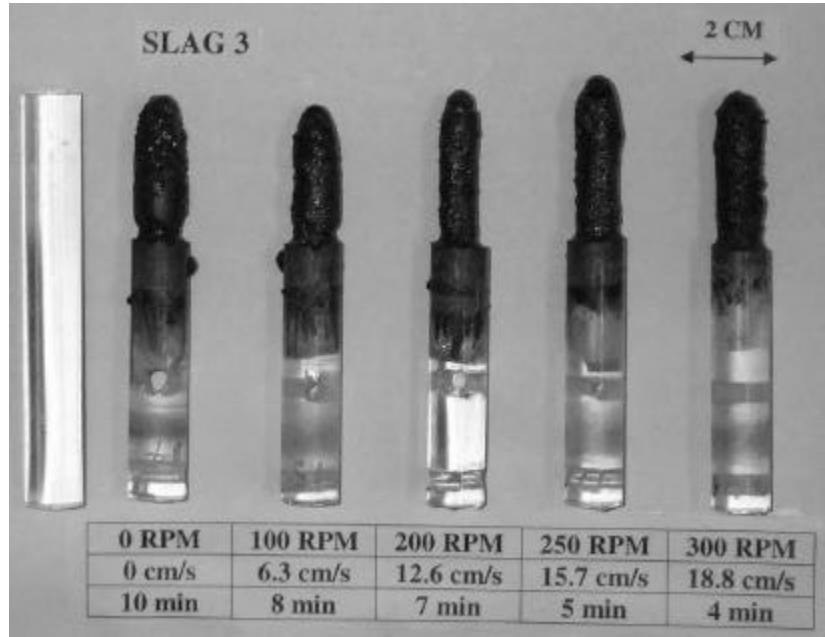
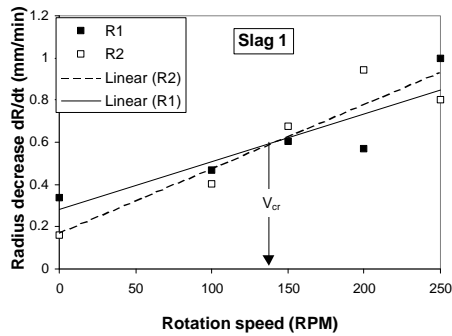
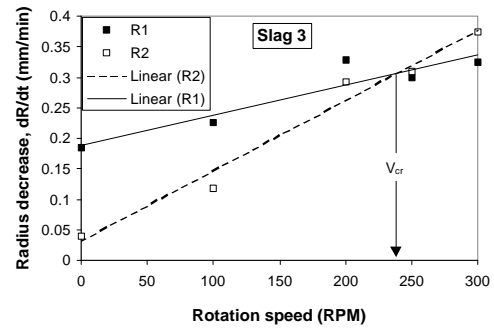


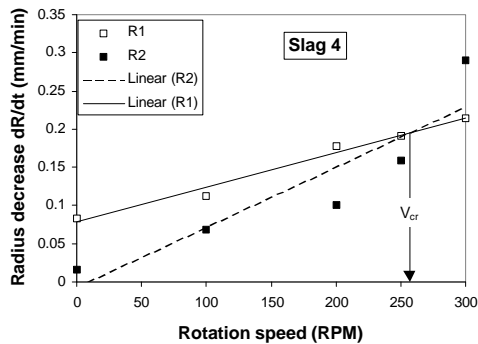
Figure 3. Digital image of side view of silica rods immersed in Fe-saturated silicate slag at 1300°C. Rotation speed and duration of the experiment are also shown.



(a)



(b)



(c)

Figure 4. Measured rate of radius decrease for Fe-saturated slags at 1300°C, as a function of rotation speed. Using a linear regression analysis, the interception point gives critical rotation velocity values of V_{cr} 8.8, 15.0 and 16.2 cm/s for slags 1(a), 3(b) and 4(c), respectively.

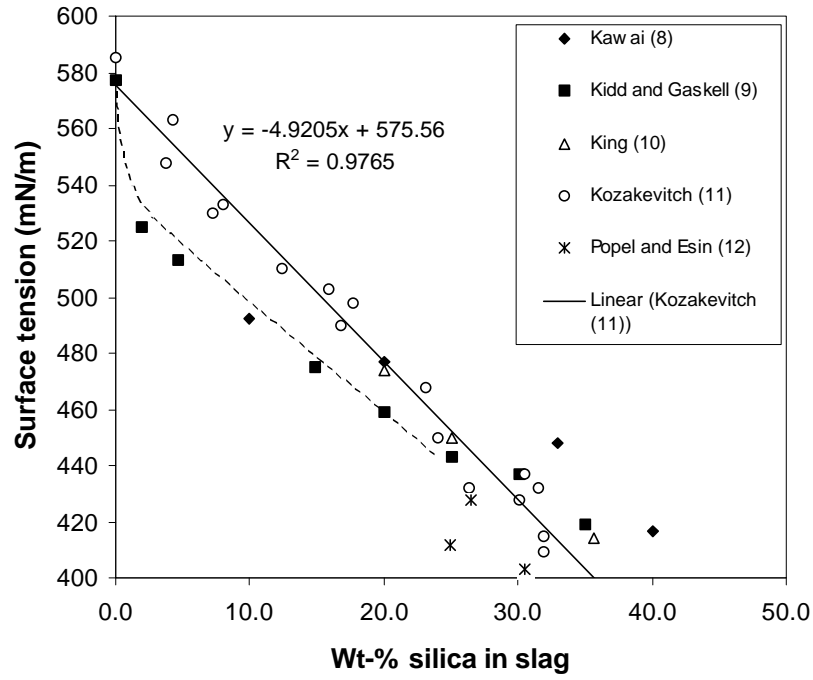


Figure 5. The variation of the surface tension of iron saturated silicate slag, with increasing silica content⁷⁻¹²⁾.

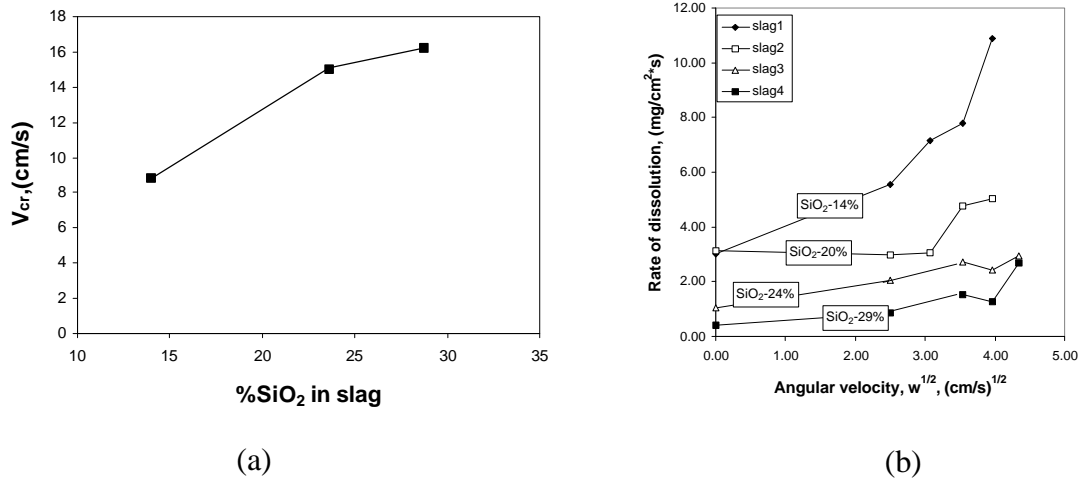
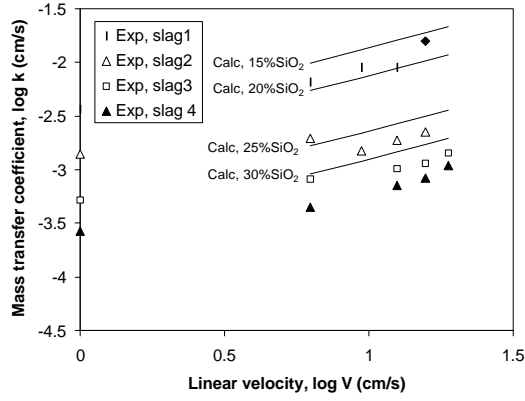
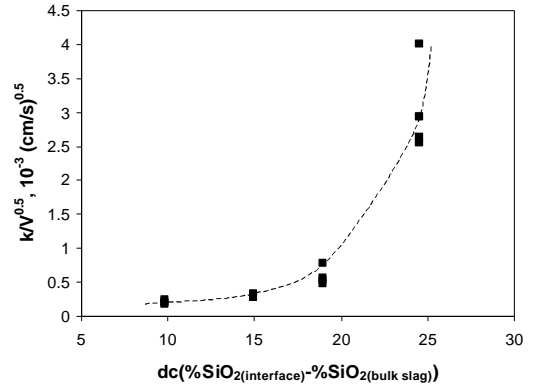


Figure 6. a) Relationship between critical melt velocity, V_{cr} , and concentration of surface active agent in slag, wt-% SiO_2 , and b) silica dissolution rate in Fe-saturated silicate slag at 1300°C as a function of rotation speed of 0, 100, 150, 200, 250 and 300 RPM.

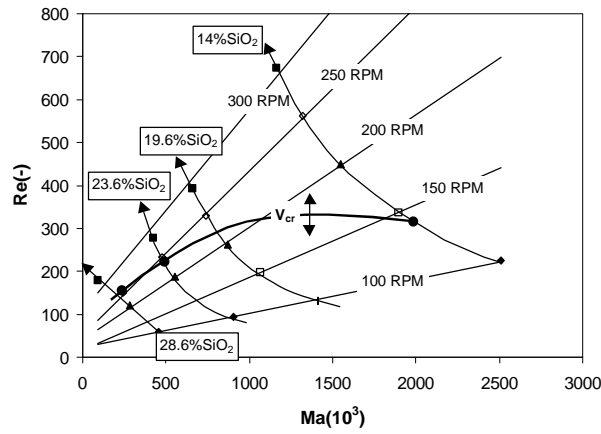


(a)

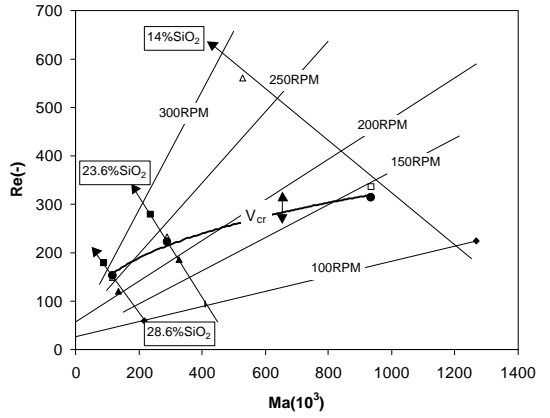


(b)

Figure 7. (a) Calculated and experimental mass transfer coefficients as a function of rotation speed and slag silica composition and (b) experimental mass transfer coefficient and rotation velocity as a function of silica concentration gradient between bulk slag and sample surface.



a)



b)

Figure 8. Effect of Marangoni convection, rotation velocity and silica content of slag on Reynolds number. a) Calculated $k^{13)}$ and b) experimentally determined k .

Table I. *Slag compositions: raw materials, and chemical analysis*

Calculated composition				Chemical analysis*				
Slag	FeO	Fe ₂ O ₃	SiO ₂	FeO	Fe ₂ O ₃	SiO ₂	Fe/SiO ₂	Fe ₂ O ₃ /FeO
1	80	5	15	79.1	6.9	14.0	4.76	0.09
2	75	5	20	74.0	6.4	19.6	3.17	0.09
3	70	5	25	71.8	4.6	23.6	2.51	0.06
4	65	5	30	68.2	3.1	28.7	1.92	0.05

* Samples were run using a Varian Vista AX ICP AES instrumental procedure. The method used for ferrous iron is semi quantitative, which means that the relative error associated with it is around 10-20%. Ferric iron concentration is estimated from the difference between the total and the ferrous iron concentrations.

Table II. *Values of mass transfer coefficient and thickness of boundary layer with rotation speed of 100 rpm.*

<u>Slag</u>	<u>k (cm/s)</u>	<u>δ (cm)</u>
<i>1</i>	6.642E-03	7.53E-04
<i>2</i>	1.961E-03	2.55E-03
<i>3</i>	8.228E-04	6.08E-03
<i>4</i>	4.444E-04	1.125E-02